25 Radiative Decay Engineering: Metal-Enhanced Fluorescence

In the preceding chapters we described the wide-ranging applications of fluorescence. All these applications relied upon the spontaneous emission of fluorophores in free space. By free space we mean optically transparent nonconducting media. In these final chapters we describe a new topic called radiative decay engineering (RDE). The term RDE is used because the environment around the fluorophore is modified or engineered to change the radiative decay rate of the fluorophore. In Chapter 1 we showed that the radiative decay rate (Γ) is determined by the extinction coefficient of the fluorophore. Extinction coefficients do not change substantially in different environments. Similarly, the radiative rates remain nearly the same under most conditions. The changes in quantum yield or lifetime displayed by fluorophores in different environments are due to changes in the non-radiative decay rates.

In this chapter we describe the effects of conducting metallic silver particles on fluorescence. A fluorophore in the excited state has the properties of an oscillating dipole. The excited fluorophore can induce oscillations of the electrons in the metal. The electric field created by the metal can interact with the excited fluorophore and alter its emission. This interaction is almost certainly bidirectional so that light-induced oscillations in the metal can affect the fluorophore. The interactions of fluorophores with metallic surfaces can have a number of useful effects, including increased quantum yields, increased photostability, increased distances for resonance energy transfer, and decreased lifetimes. These changes can result in increased sensitivity, increased photostability, and decreased interference from unwanted background emission. These effects are called metal-enhanced fluorescence (MEF).

The mechanisms of metal-enhanced fluorescence are not yet completely understood, and the applications of MEF are just beginning. Because of the potential importance of RDE and MEF we decided to include chapters on these topics. This is a new topic and the field is changing very rapidly. Hence this chapter represents a summary of the current knowledge in this field. RDE and MEF were developed in this laboratory, and as a result many of the examples are from our own work.

25.1. RADIATIVE DECAY ENGINEERING

Prior to describing the unusual effects of metal surfaces on fluorescence it is valuable to describe what we mean by RDE and in particular spectral changes expected for increased radiative decay rates.

25.1.1. Introduction to RDE

We typically perform fluorescence measurements in macroscopic solutions, or at least macroscopic in comparison with the size of a fluorophore. The solutions are typically transparent to the emitted radiation. There may be modest changes in refractive index, such as for a fluorophore in a membrane, but such changes have a relatively minor effect on the fluorescence spectral properties.[1–2] In such nearly homogeneous solutions, the fluorophores emit into free space and are observed in the far field. Local effects due to surfaces are not usually observed because of the small size of fluorophores relative to the experimental chamber. The spectral properties of a fluorophore in the excited state are well described by Maxwell's equations for an oscillating dipole radiating into free space and we detect the far-field radiation as light.

For clarity we note that we are not considering reflection of the emitted photons from the metal surfaces. Reflection occurs after emission. We are considering the effects of the nearby surface on altering the "free space" condition, and modifying Maxwell's equation from their free space counterparts.[3–4] Like a radiating antenna, a fluorophore is an oscillating dipole, but one that oscillates at high frequency and radiates short wavelengths. Nearby metal surfaces can respond to the oscillating dipole and modify the rate of emission and the spatial distribution of the radiated energy. The electric field felt by a fluorophore is affected by interactions of the incident light with the nearby metal surface and also by interaction of the fluorophore oscillating dipole with the metal surface. Additionally, the fluorophores oscillating dipole induces a field in the metal. These interactions can increase or decrease the field incident on the fluorophore and increase or decrease the radiative decay rate.

For simplicity we will refer to metallic particles as metals. At first glance it seems unusual to consider using metallic surfaces to enhance fluorescence. Metals are known to quench fluorescence. For example, silver surfaces 50 Å thick are used in microscopy to quench emission from regions near the metal.[5] We now know that metals can also enhance fluorescence by several mechanisms. The metal particles can cause increased rates of excitation due to a more concentrated electric field around the particle. Metals also appear to increase the rates of radiative decay (Γ). We will describe the effects of metallic particles on fluorescence as if an increase in Γ is a known fact. However, the physics is complex and it is not always clear what is emitting the light: the fluorophore or the metal.

Prior to describing RDE in more detail it is informative to see a result. Figure 25.1 shows a photograph of a microscope slide that is coated with fluorescein-labeled human serum albumin. The left side of the slide has no metal. The right side of the slide is covered with silver particles. The fluorescein molecules near the metal particles are remarkably brighter. Similar effects have now been observed for many different fluorophores, showing that MEF is a general effect.

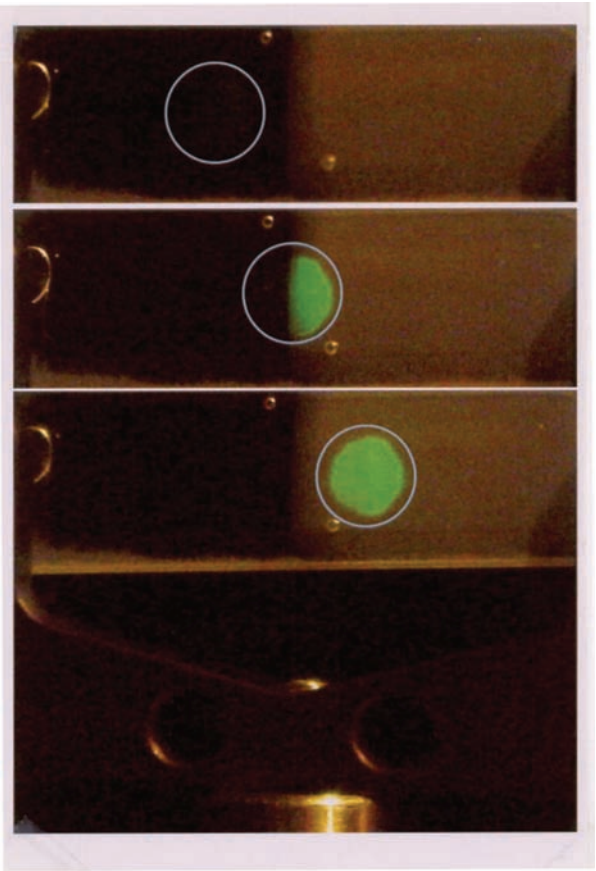

Figure 25.1. Effect of metallic silver particles on surface-bound fluorescein-labeled human serum albumin. Left, no silver; right, with silver particles.

25.1.2. Jablonski Diagram for Metal-Enhanced Fluorescence

An increase in the radiative decay rate can have unusual effects on fluorophores.[6] These effects can be understood by considering a Jablonski diagram that includes MEF (Figure 25.2). For simplicity we will only consider radiative decay (Γ) and non-radiative decay (k_{nr}). In the absence of metals the quantum yield and lifetimes are given by

$$Q_0 = \Gamma/(\Gamma + k_{nr}) \tag{25.1}$$

$$\tau_0 = (\Gamma + k_{nr})^{-1} \tag{25.2}$$

Since the radiative decay rate is nearly constant for any fluorophore the quantum yield can only be increased by decreasing the value of k_{nr}.

Now consider the effect of a metal. If the metal results in an increased rate of excitation ($E + E_m$) this will result in increased brightness without changing the quantum yield or lifetime. This is a useful effect that can allow decreased incident intensities and decreased background. Metal-enhanced excitation can also result in selective excitation of fluorophores near the metal. Another possible effect is an increase in the radiative decay rate. In this case the quantum

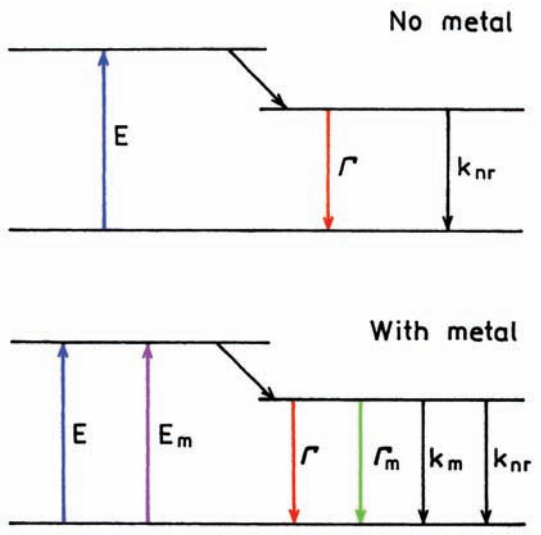

Figure 25.2. Jablonski diagram without (top) and with (bottom) the effects of near metal surfaces. E is the rate of excitation without metal. E_m is the additional excitation in the presence of metal [6].

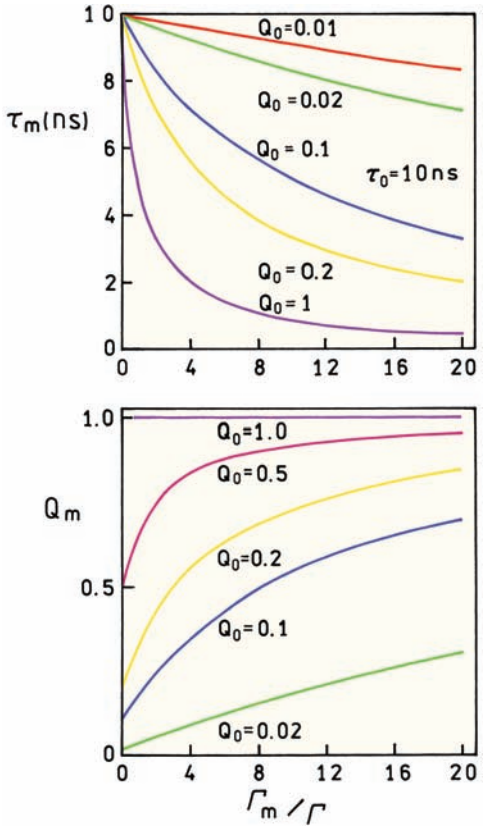

Figure 25.3. Effect of an increase in the metal-induced radiative rate on the lifetime and quantum yields of fluorophores. For $Q = 0.5$, $\Gamma = 5 \times 10^7$/s and $k_{nr} = 5 \times 10^7$/s. For $Q = 0.1$, $\Gamma = 1 \times 10^7$/s and $k_{nr} = 9 \times 10^7$/s. From [6].

yield and lifetime of the fluorophore near the metal surface are given by

$$Q_m = \frac{\Gamma + \Gamma_m}{\Gamma + \Gamma_m + k_{nr}} \tag{25.3}$$

$$\tau_m = (\Gamma + \Gamma_m + k_{nr})^{-1} \tag{25.4}$$

These equations result in unusual predictions for a fluorophore near a metal surface. As the value of Γ_m increases the quantum yield increases while the lifetime decreases.

The effects of increasing Γ_m are shown in Figure 25.3. The x-axis is the relative value between the radiative decay rate due to the metal (Γ_m) and the rate in the absence of metal (Γ). As Γ_m increases the lifetime decreases. A decrease in lifetime is usually associated with a decrease in quantum yield. However, this is because a decrease in lifetime is usually due to an increase in k_{nr}. When the total decay rate, $\Gamma_T = \Gamma + \Gamma_m$, increases the quantum yield increases. This increase occurs because more of the fluorophores emit before they can decay through the non-radiative pathway. The effect is larger for fluorophores with low quantum yields because increasing Γ_m has no effect on Q if it is already unity.

25.2. REVIEW OF METAL EFFECTS ON FLUORESCENCE

There is extensive physics literature on the interaction of fluorophores with metal surfaces and particles, much of it theoretical.[7–12] The possibility of altering the radiative decay rates was experimentally demonstrated by measurements of the decay times of a europium (Eu^{3+}) complex positioned at various distances from a planar silver mirror.[13–16] In a mirror the metal layer is continuous and thicker than the optical wavelength. The lifetimes oscillate with distance but remain a single exponential at each distance (Figure 25.4). This effect can be explained by changes in the phase of the reflected field with distance and the effects of this reflected near-field on the fluorophore. The changes in lifetime with distance are not due to interactions of the fluorophore with emitted photons. A decrease in lifetime is found when the reflected field is in phase with the fluorophore's oscillating dipole. An increase in the lifetime is found if the reflected field is out of phase with the oscillating dipole. As the distance increases the amplitude of the oscillations decreases. The effects of a plane mirror occurs

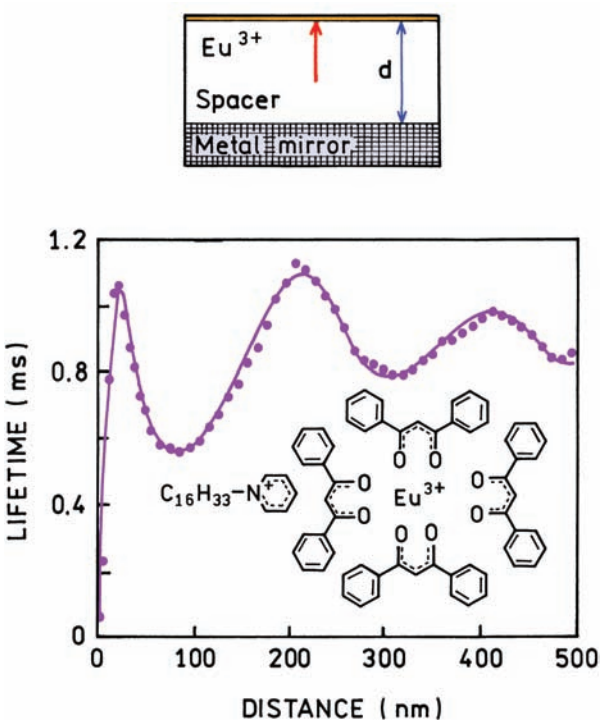

Figure 25.4. Lifetime of Eu^{3+} ions in front of an Ag mirror as a function of separation between the Eu^{3+} ions and the mirror. The solid curve is a theoretical fit. From [6].

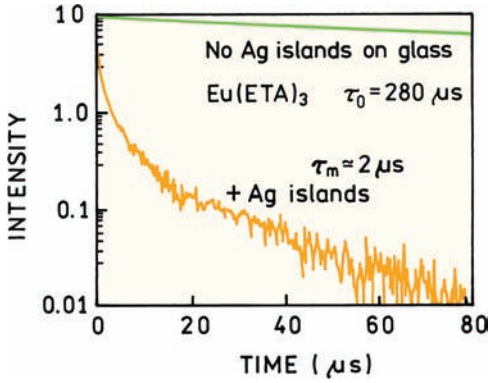

Figure 25.5. Fluorescence decay of $Eu(ETA)_3$ on silver-island films. Eu^{3+} was complexed with thenoyltrifluoroacetonate (ETA). From [6].

over distances comparable to the excitation and emission wavelengths. At short distances below 20 nm the emission is quenched. The oscillations in lifetime with distance from the metal surface are rather modest. These effects have been of theoretical interest but have not found use in the applications of fluorescence.

The effects of metallic surfaces on optical spectra are strongly dependent on the nature of the metal surface and/or metal particles. In general more dramatic effects are observed for metal colloids than planar mirrored surfaces. The experiment that led to our interest in RDE is shown in Figure 25.5. A glass slide was coated with silver island films (SIFs). These films are a partial coating of the surface with sub-wavelength size silver particles, which are formed by chemical reduction. The surface was coated with $Eu(ETA)_3$. The intensity decays were measured in the absence and presence of an SIF. The lifetime of $Eu(ETA)_3$ decreased more than 100-fold on the SIF.[17] At first this decrease in lifetime did not seem interesting to us because we thought it could be due to quenching or scattered light giving the appearance of a shorter lifetime. However, the intensity increased fivefold even though the lifetime was decreased 100-fold. To the best of our knowledge these results can only be explained by an increase in the radiative decay rate. This increase in Γ must be 100-fold or greater. This result suggested the metal particles could be used to modify or control the radiative rates of fluorophores. The magnitude of the effect was large, which suggested the use of metal particles to increase the sensitivity of fluorescence detection.

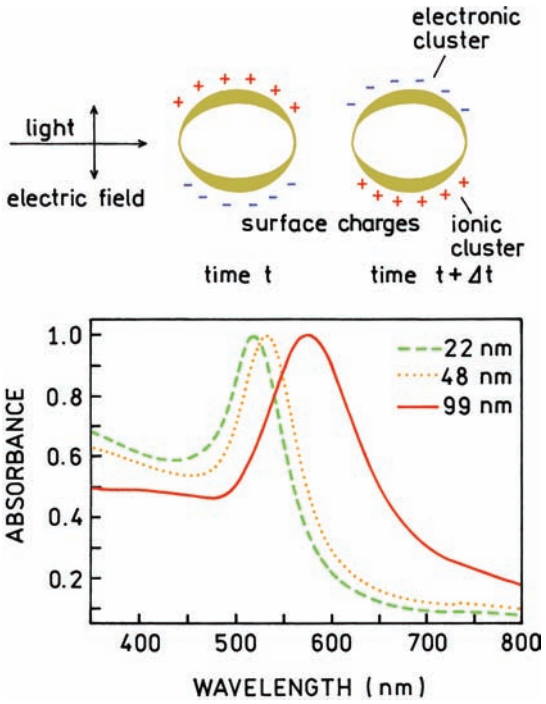

Figure 25.6. Electron oscillations in a metal colloid induced by incident light. Revised and reprinted with permission from [22]. Copyright © 1999, American Chemical Society.

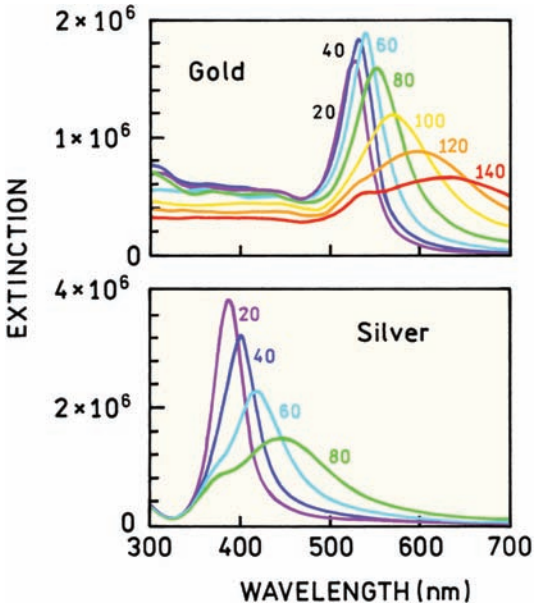

Figure 25.7. Extinction spectra of gold and silver colloids. Revised and reprinted with permission from [22]. Copyright © 1999, American Chemical Society.

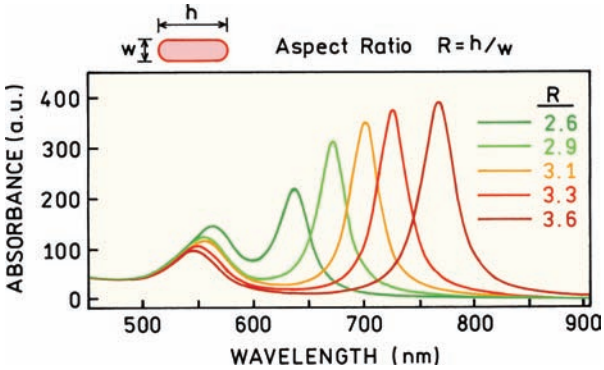

Figure 25.8. Absorption spectra of gold rods with different aspect ratios. From [22].

25.3. OPTICAL PROPERTIES OF METAL COLLOIDS

Metal colloids have been used for centuries to make some colored glasses.[18] However, the origin of the colors was not understood until 1857, when Faraday discovered that the colors were due to finely divided silver or gold particles.[19] Incident light interacts with small metal particles and induces electron oscillations (Figure 25.6).[20–22] The oscillating field can generate far-field radiation at the same wavelength. The result is that the incident light is scattered by the colloids, so the glass appears the of color the unscattered light. The actual situation is a little more complex in that colloids can also absorb light.

Extinction spectra of silver and gold colloids are shown in Figure 25.7. The term extinction refers to attenuation of the light as it goes through the sample. The extinction is due to both absorption and scattering. We will occasionally use the term "absorption" to refer to extinction. The extinction shifts to longer wavelengths as the size of the colloids increases.[23–27] Gold colloids absorb at longer wavelengths than silver colloids. The absorption depends strongly on colloid shape. This effect is seen by the shift in the absorption spectrum of gold colloids as they become elongated (Figure 25.8).

The unusual spectral properties of colloids can be seen by visual observation. Figure 25.9 shows absorption spectra

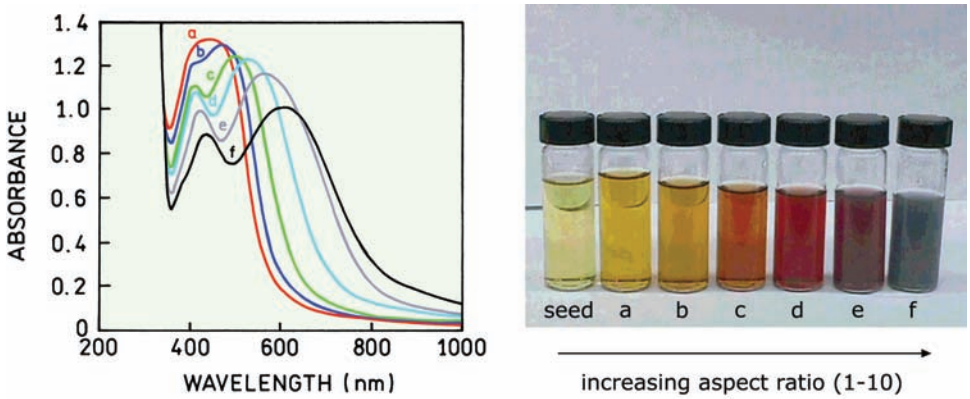

Figure 25.9. Extinction spectra and photograph of suspensions of silver colloids. The aspect ratios increase from left to right. Reprinted with permission from [23].

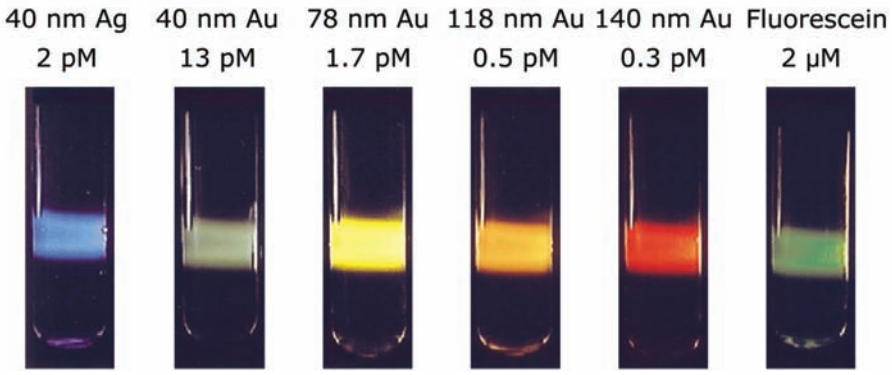

Figure 25.10. Photographs of colloid suspensions when illuminated from the side with white light. The rows of numbers indicate the diameter and concentration of the colloids. The rightmost sample is fluorescein. Reprinted with permission from [24-25].

and a backlit photo of silver colloid suspensions.[23] The aspect ratio increases from left to right and the perceived color changes with aspect ratio. A different result is seen if the samples are illuminated from the side without a backlight (Figure 25.10). These samples give the appearance of being fluorescent. The rightmost sample is fluorescent but the others are not. These samples are illuminated with a beam of white light. The perceived color is the color that is scattered by the colloids. The smallest silver colloids scatter blue light and the largest gold colloids scatter red light.

Samples that scatter light usually have a turbid appearance. However, the colloid suspensions in Figure 25.9 and 25.10 are clear. This occurs because the colloids are extremely dilute. Colloids have a large cross-section for interacting with light and extinction coefficients on the order of 10^{10} or 10^{11} M^{-1} cm^{-1}. The cross-section for a strongly absorbing chromophore like fluorescein is 2.0 x 10^{-15} cm^2 or 4.5 Å across, which is about the size of the molecule. The cross-section for a 60-nm silver colloid is 1.4 x 10^{-10} cm^2 or 1000 Å across. Only a low density of colloids is needed to cause enough scattering to change the color. Because of this high optical cross-sections colloids are being used to develop a number of bioaffinity assays.[26–33]

25.4. THEORY FOR FLUOROPHORE–COLLOID INTERACTIONS

A complete explanation of fluorophore–colloid interactions would require extensive electrodynamic theory, and the description would probably still be incomplete. We will describe an overview of those results that are relevant to MEF. The details are not known with certainty, but there probably are three dominant interactions of fluorophores with metals (Figure 25.11). Fluorophores may be quenched at short distances from the metal (k_m), but there may be ways to recover this energy as useful emission (Chapter 26). There can be an increased rate of excitation (E_m), which is called the lightening-rod effect, and there can be an increased rate of radiative decay (Γ_m). The distance of the interactions probably increases, in order, with quenching, increased excitation, and increased radiative rate. However, additional experimental results are needed to better determine the distance dependence of these interactions.

The interactions between fluorophores and metal colloids have been considered theoretically.[7–12] A typical model is shown in Figure 25.12 for a prolate spheroid with an aspect ratio of *a/b*. The particle is assumed to be a metal-

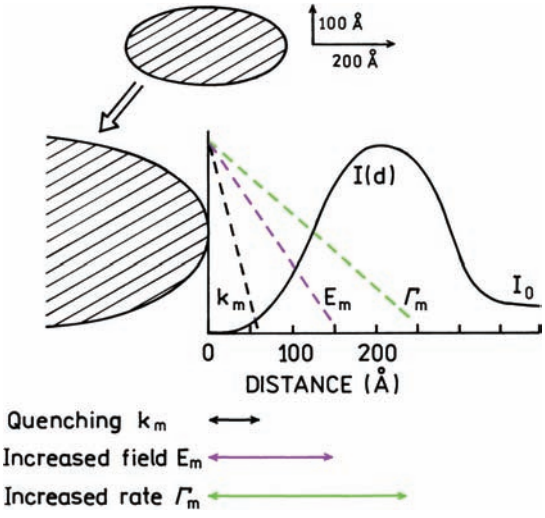

Figure 25.11. Effects of a metallic particle on transitions of a fluorophore. Metallic particles can cause quenching (k_m), can concentrate the incident light field (E_m), and can increase the radiative decay rate (Γ_m). From [6].

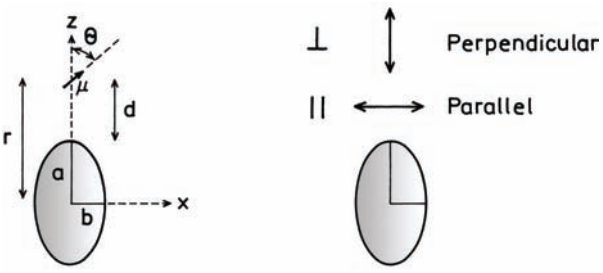

Figure 25.12. Fluorophore near a metallic spheroid.

lic ellipsoid with a fluorophore positioned near the particle. The fluorophore is located outside the particle at a distance r from the center of the spheroid and a distance d from the surface. The fluorophore is located on the major axis and can be oriented parallel or perpendicular to the metallic surface.

The theory can be used to calculate the effect of the metal particle on a nearby fluorophore. Figure 25.13 shows the radiative rates expected for a fluorophore at various distances from the surface of a silver particle and for different orientations of the fluorophore transition moment. The most remarkable effect is for a fluorophore aligned along the long axis and perpendicular to the surface of a spheroid with an aspect ratio of a/b = 1.75. In this case the radiative rate can be enhanced by a factor of 1000-fold or greater. The effect is much smaller for a sphere (a/b = 1.0) and for a more elongated spheroid (a/b = 3.0). For this elongated particle the optical transition is not in resonance with the fluorophore. In this case the radiative decay rate can be decreased by over 100-fold. If the fluorophore displays a high quantum yield or a small value of k_{nr}, this effect could result in longer lifetimes. The magnitude of these effects depends on the location of the fluorophore around the particle and the orientation of its dipole moment relative to the metallic surface. The dominant effect of the perpendicular orientation is thought to be due to an enhancement of the local field along the long axis of the particle.

Colloids can also affect the extent of resonance energy transfer.[34–35] Suppose the donor and acceptor are located along the long axis of an ellipsoid with the dipoles also oriented along this axis. Figure 25.14 shows enhancement of the rate of energy transfer due to the metal particle, that is, the ratio of the rates of transfer in the presence (k_T^m) and absence (k_T^0) of the metal. Enhancements of 10^4 are possible. The enhancement depends on the transition energy that is in resonance with the particle. A smaller but still significant enhancement is found for a less resonant particle (lower curve). The enhanced rate of energy transfer persists for distances much larger than typical Förster distances. These simulations are for dipoles on the long axis and oriented along that axis, but the enhancements are still large

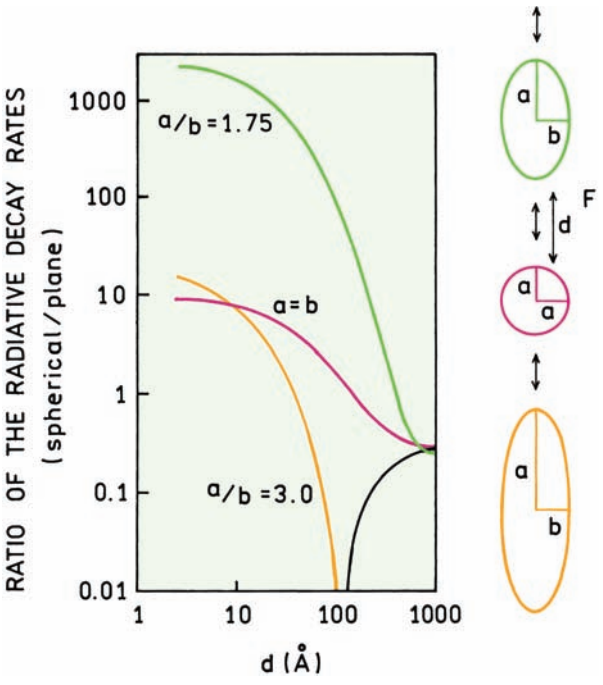

Figure 25.13. Effect of a metallic spheroid on the radiative rate of a fluorophore. The resonant frequency of the dye is assumed to be 25,600 cm^{-1}, approximately equal to 391 nm. The volume of the spheroids is equal to that of a sphere with a radius of 200 Å.

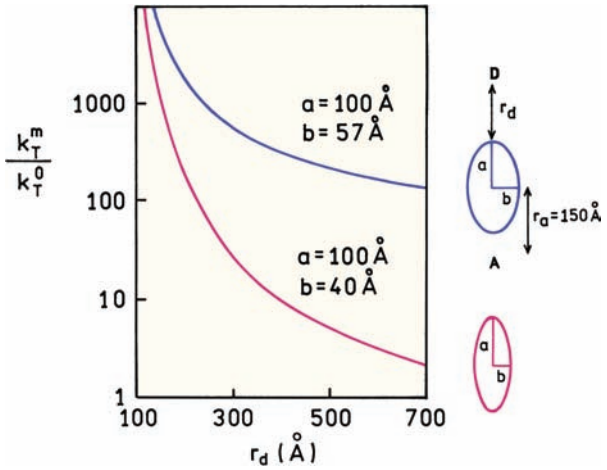

Figure 25.14. Enhancements in the rate of energy transfer in the presence of silver particle.

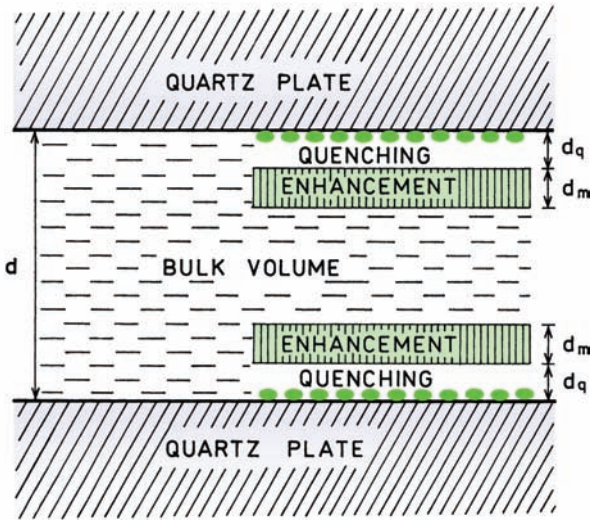

Figure 25.15. Schematic for a fluorophore solution between two silver island films. The solid ellipsoids represent the silver island films.

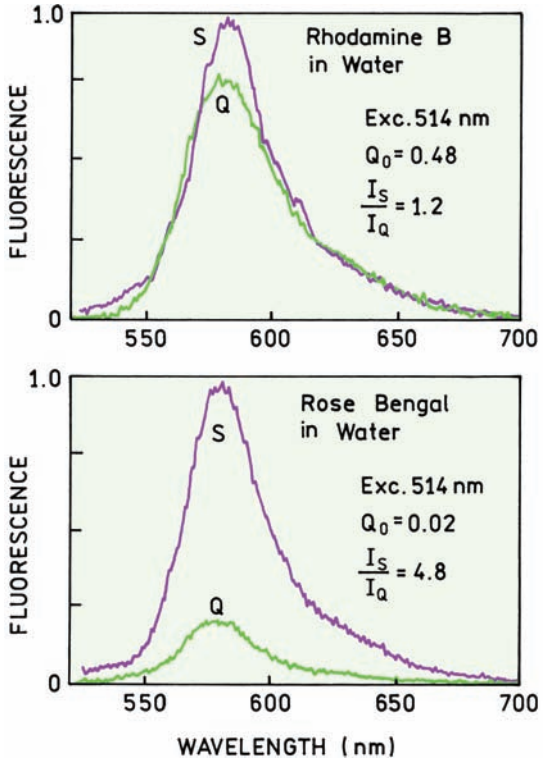

Figure 25.16. Emission spectra of rhodamine B (top) and rose bengal (bottom) between silver island films (S) or unsilvered quartz plates (Q). From [36].

when the donors and acceptors have different orientations and locations around the particle.

25.5. EXPERIMENTAL RESULTS ON METAL-ENHANCED FLUORESCENCE

Prior to describing biochemical applications of MEF it is informative to see the effects of silver particles on standard fluorophores. Silver island films are deposited on glass or quartz plates. Two plates are put together with water in between, yielding a sample about 1 μm thick (Figure 25.15). With this sample most of the volume is distant from the silver and thus not affected by the silver. Fluorophores with high and low quantum yields were placed between the SIFs.[36] As shown in Figure 25.3, an increase in the radiative decay rate increases the intensity when the quantum yield is low but will not affect the intensity of a high-quantum-yield fluorophore. For this reason we examined two fluorophores, with high or low quantum yields. The intensity of rhodamine B (RhB) with a quantum yield of 0.48 is (Figure 25.16) almost unchanged by the SIFs. In contrast, the intensity of rose bengal (RB) with a quantum yield of 0.02 is increased about fivefold by proximity to the silver island films. In this sample the fluorophores are not attached to the silver and most of the fluorophores are too distant from the silver to be affected. Hence the intensity increase of those RB molecules near the metal film is significantly greater than fivefold.

Metal-enhanced fluorescence by SIFs is a general phenomenon that appears to occur with most if not all fluorophores. Figure 25.17 shows the relative intensities in the presence (I_S) and absence (I_Q) of metal for the fluorophores. If the quantum yield is above 0.5 the intensity is not significantly increased between the SIFs. As the quantum yield decreases the intensity ratio I_S/I_Q increases. This result is consistent with an increase in the radiative decay rate near the SIFs. Fluorophores with a variety of structures were examined so that the effect is unlikely to be the result of some specific interactions of a fluorophore with the silver.

25.5.1. Application of MEF to DNA Analysis

DNA analysis is a widely used application of fluorescence, and MEF can be used to obtain increased intensities from labeled DNA.[36–40] Figure 25.18 shows the chemical structures of DNA oligomers labeled with Cy3 or Cy5. These fluorophores are frequently used on DNA arrays. The glass or quartz substrate from these arrays is often treated with 3-aminopropyltriethoxysilane (APS), which makes the sur-

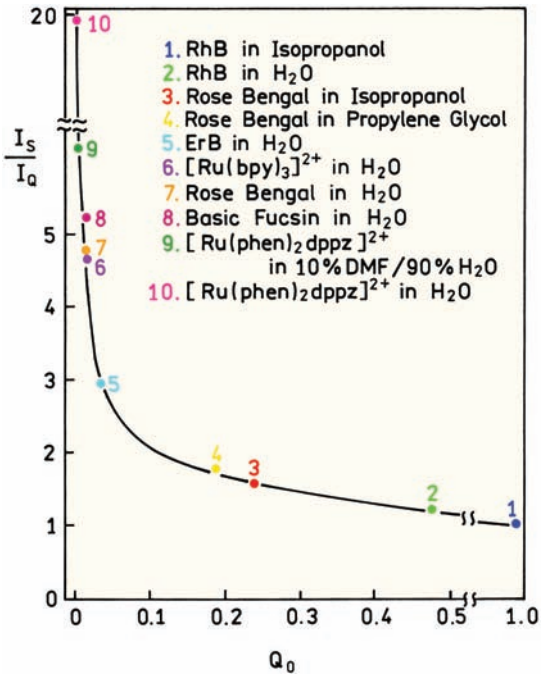

Figure 25.17. Enhancement of the emission of fluorophores with different quantum yields. From [36].

face positively charged for DNA binding. The emission intensity of both oligomers is increased about fourfold when bound to the SIFs as compared to quartz (Figure 25.19).

The previous figures showed that the intensities of fluorophores increased when near SIFs. However, fluorescence intensities can change for many reasons, and it would not be surprising if surface-bound fluorophores in a rigid environment displayed higher intensities than in solution,. As shown in Figure 25.3, an increase in the radiative decay rate will decrease the lifetime, as will increasing quantum yield. This is an unusual effect so that lifetime measurements can be used to determine if the radiative decay rate is increased near the metal. Figure 25.20 shows frequency-domain (FD) intensity decays of the labeled oligomers when bound to quartz and SIFs. The mean lifetimes of Cy3 and Cy5 are decreased dramatically on the SIFs. The decreased lifetimes and increased intensities show that the radiative decay rate increased near the SIFs. The right-hand panels show the intensity decays reconstructed from the FD data. These curves show an initial rapid decay followed by a slower decay comparable to that found for the labeled DNA on glass. In this case the more slowly decaying components are probably due to labeled DNA bound to the glass but distant from the metal particles.

A decrease in lifetime should result in increased photostability of a fluorophore. Photochemical reactions occur while the fluorophore is in the excited state. If the lifetime is shorter, it is more probable that the fluorophore emits before it undergoes decomposition. This means that the fluorophore can undergo more excitation–relaxation cycles prior to permanent photobleaching. This reasoning assumes

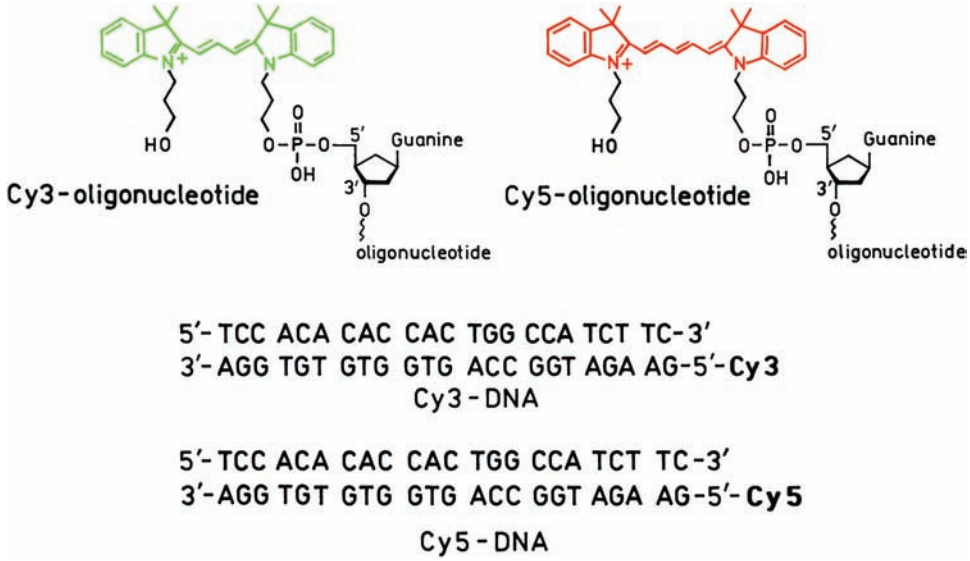

Figure 25.18. Structure of DNA oligomers labeled with Cy3 or Cy5. From [37].

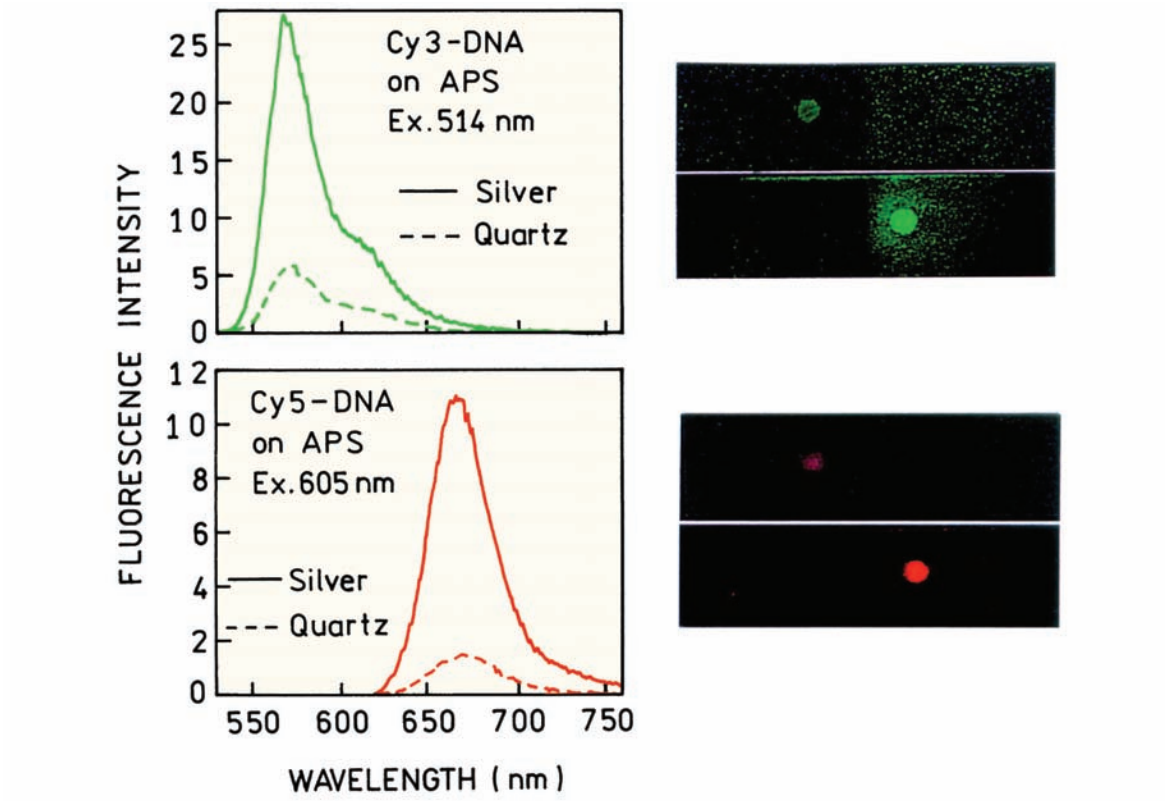

Figure 25.19. Emission spectra and photographs of the labeled DNA oligomer on quartz and SIFs. The quartz was treated with APS. From [40].

that the metal does not introduce a new pathway for photodecomposition. The photostability of a fluorophore can be studied by measuring the intensity with continuous excitation (Figure 25.21). These photostability curves for Cy3- and Cy5-labeled DNA were measured with the same incident light intensity, so that the initial intensities are higher on the SIFs. The total number of photons emitted by a fluorophore prior to photobleaching is proportional to the area under the intensity-versus-time curves. These non-normalized curves (left) show that considerably more photons per fluorophore can be observed on the SIFs. If the curves are normalized at time zero (right) the fluorophores on the SIFs are seen to bleach somewhat more slowly. Results similar to those in Figure 25.21 have been observed for a number of fluorophores,[41–43] but it is too early to know if increased photostability will be observed with most fluorophores.

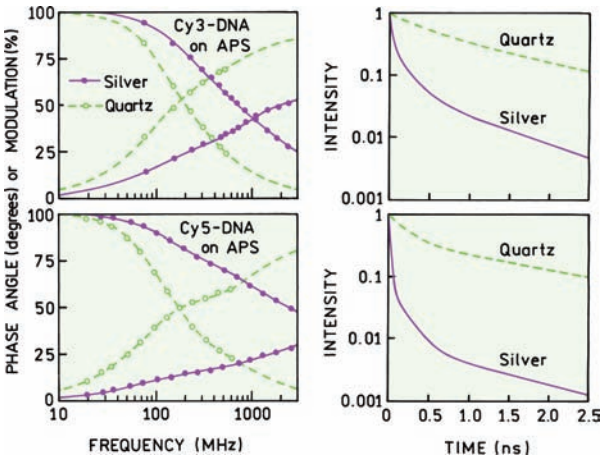

Figure 25.20. Time-dependent intensity decays of Cy3- and Cy5-labeled DNA oligomers on quartz and SIFs. From [40].

Detection of DNA using fluorescence is almost always performed using extrinsic probes. The intrinsic fluorescence of the DNA bases is very weak. Silver particles were found to increase the intrinsic fluorescence of unlabeled DNA. Figure 25.22 shows emission spectra of calf thymus DNA in solution when placed between quartz plates and when between SIFs.[44] The intensity is increased manyfold between the SIFs. In this experiment the DNA was not bound to the glass, so that most of the DNA is distant from the silver particles. This suggests that the intensity of the DNA near the silver particles is dramatically increased.

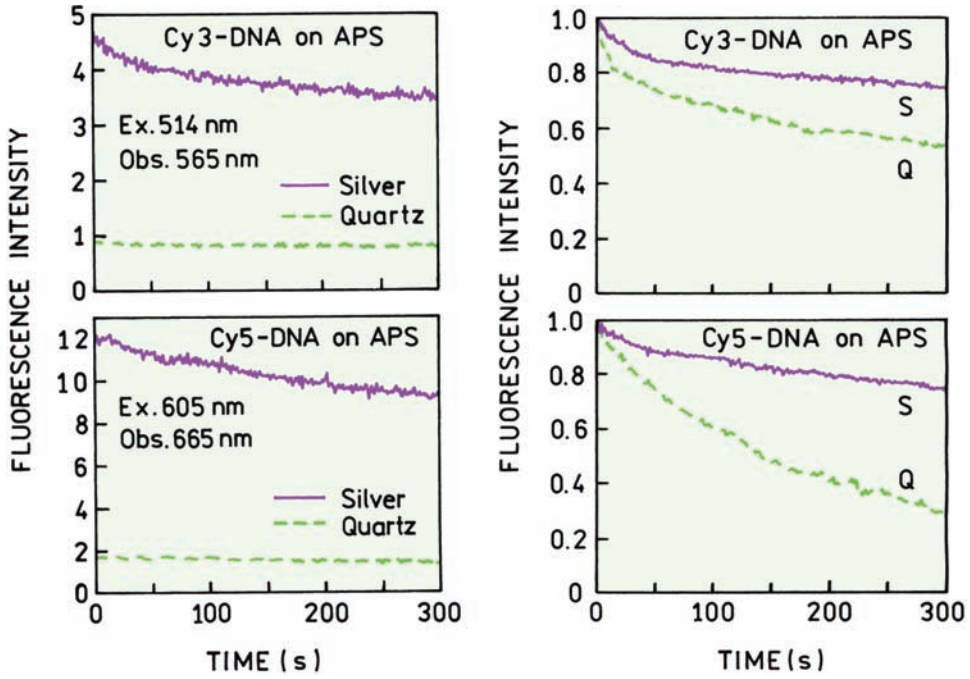

Figure 25.21. Photostability of Cy3- and Cy5-labeled DNA oligomers on quartz and SIFs. From [40].

25.6. DISTANCE-DEPENDENCE OF METAL-ENHANCED FLUORESCENCE

The use of MEF requires an understanding of the optimal distance between the fluorophore and the silver surface for enhanced fluorescence. This dependence was studied using protein layers to separate labeled DNA oligomers from the SIF.[45] The glass or SIF surface is first incubated with biotinylated bovine serum albumin (BSA). BSA adsorbs to most surfaces and forms a monolayer. The surface is then treated with avidin, which forms a layer on the biotinylated BSA (Figure 25.23). This process can be repeated many times, adding a thickness of about 90 Å for each layer of BSA and avidin. After the desired thickness is achieved the surface is treated with a biotinylated DNA oligomer that also contains a fluorophore (Figure 25.24).

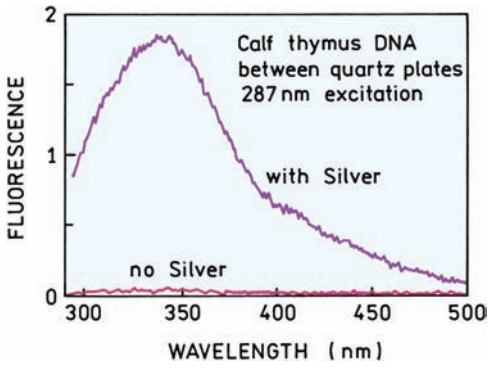

Figure 25.22. Emission spectra of calf thymus DNA between quartz plates and between SIFs.

Figure 25.25 shows the intensity of Cy3- and Cy5-labeled DNA oligomers on SIFs. The oligomers were separated from the SIF by one or more layers of BSA-avidin. The highest intensity was found with a single layer of BSA-avidin. Hence a distance of about 90 Å from a metal appears to yield the largest increases in intensity. This result is only an initial attempt to identify the optimal distances, and additional studies are needed to determine the range of distances that can be used for MEF. It should be recognized that the experimental studies of MEF shown above were performed using fluorophores that were distributed evenly across the surfaces and not localized exclusively on the metal.

25.7. APPLICATIONS OF METAL-ENHANCED FLUORESCENCE

Metal-enhanced fluorescence is a new technology, and the applications are now being developed.[46–49] We will describe a few initial results indicating the types of applications that can be expected in the near future.

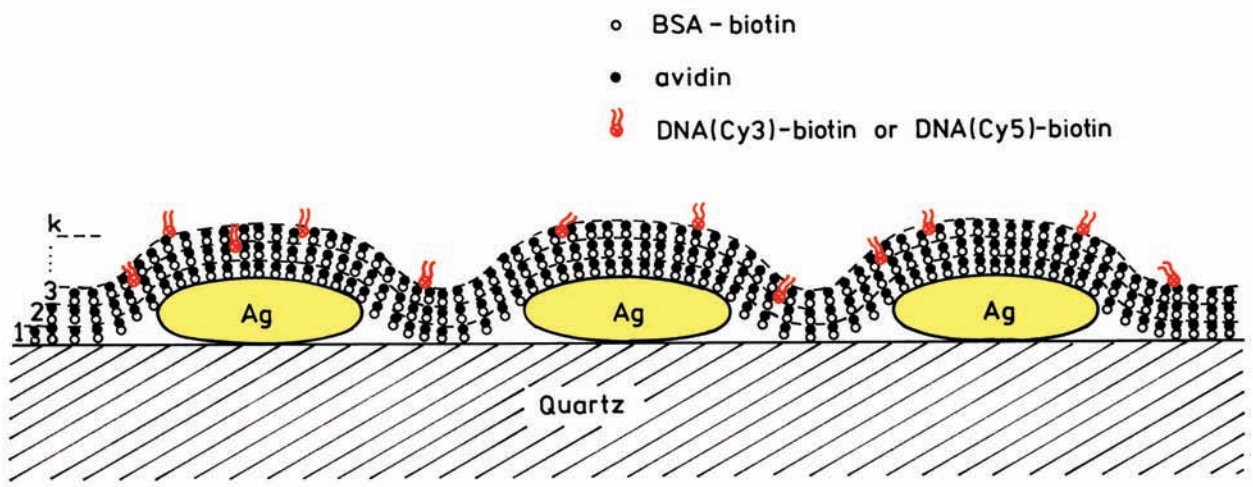

Figure 25.23. Schematic of SIFs with layers of biotinylated BSA, avidin and a top layer of labeled DNA oligomers. From [45].

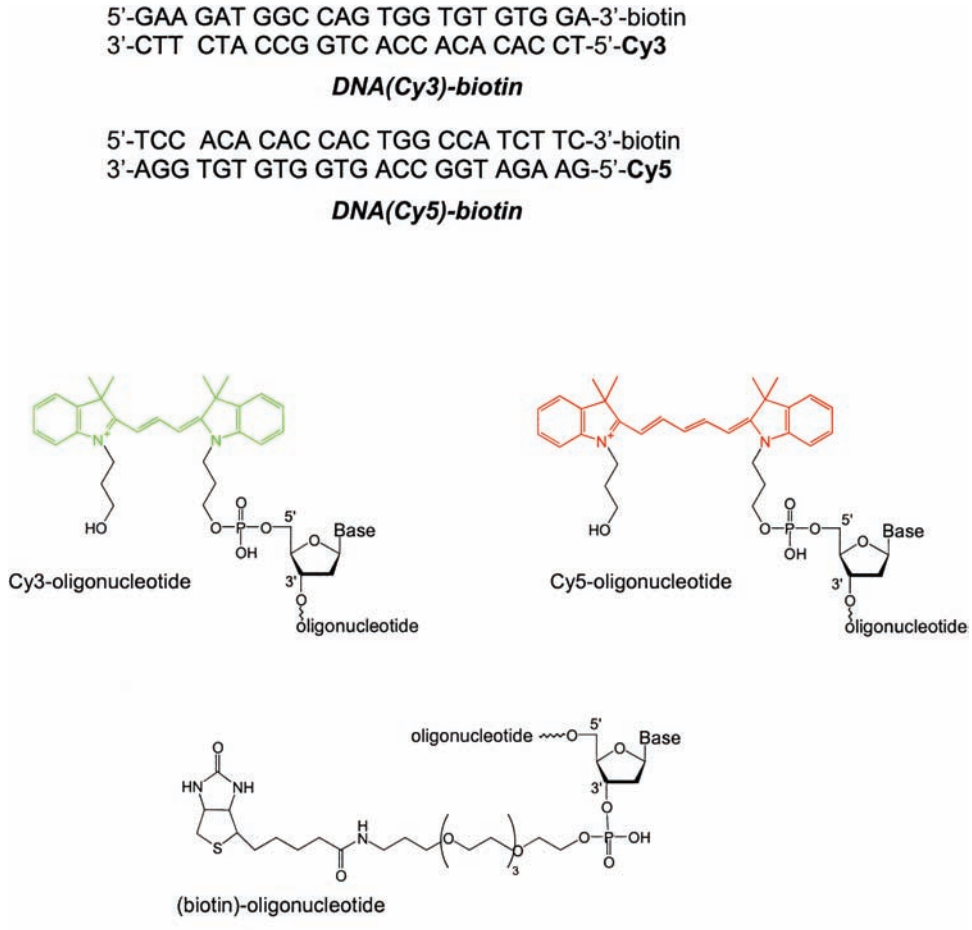

Figure 25.24. Structure of labeled and biotinylated DNA oligomers. From [45].

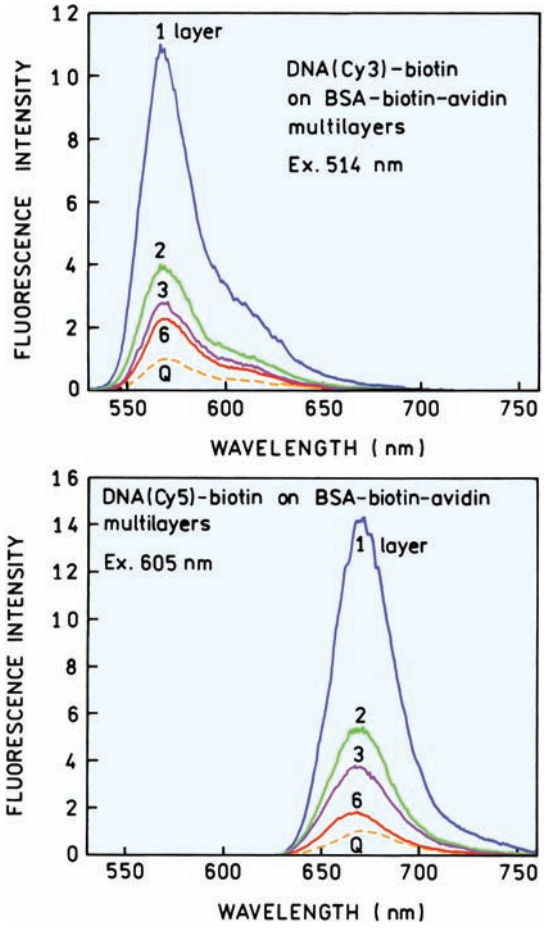

Figure 25.25. Effect of distance from the SIFs on the intensities of labeled DNA oligomers. From [45].

25.7.1. DNA Hybridization Using MEF

DNA hybridization is frequently measured using fluorophores that display increased intensity when bound to double-helical DNA. MEF allows hybridization to be measured using fluorophores for which the quantum yield, in the absence of metal, does not change upon DNA hybridization.[50] This possibility is shown for a fluorescein-labeled oligomer (Figure 25.26). A complementary DNA oligomer was bound to an SIF. Upon addition of the labeled oligomer the fluorescein intensity showed a time-dependent increase in intensity. The intensity of fluorescein increased about 10-fold upon hybridization. The effect of the SIF on the intensity is seen in the real-color photographs of the hybridized DNA before and after hybridization (Figure 25.27). It is important to understand that the increase in intensity is not due to the effect of hybridization on quantum yield of the probe. The increase in intensity is due to the localization of the probe near the SIF. This result shows that MEF can be used to detect any binding reaction that brings a fluorophore close to an SIF. A change in intensity due to the binding event is not necessary.

25.7.2. Release of Self-Quenching

Labeled immunoglobulins are frequently used in immunoassays. When performing such assays it is desirable to have the brightest possible labeled proteins. One approach to obtaining bright reagents is to label the protein with multiple fluorophores. Unfortunately, this approach is usually not successful. When proteins are labeled with flu-

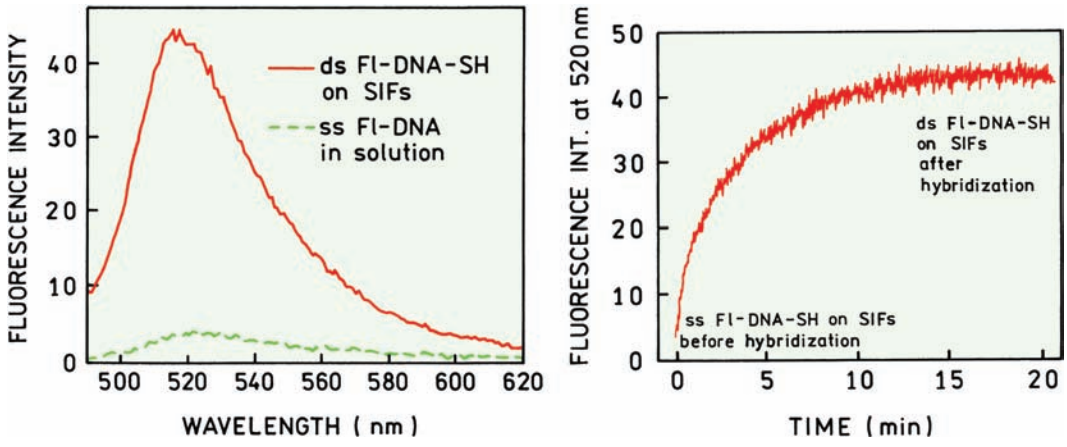

Figure 25.26. Emission spectra and time-dependent intensity of a fluorescein-labeled oligomer upon binding to a complementary oligomer bound exclusively to an SIF. From [50].

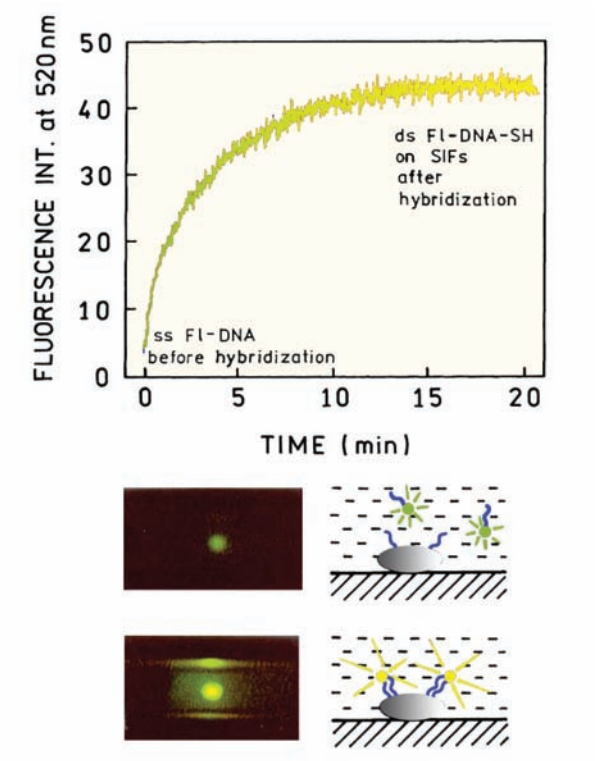

Figure 25.27. Photograph of a fluorescein-labeled DNA oligomer before (top) and after (bottom) hybridization. From [50].

orophores with a small Stokes shift the intensity does not increase in proportion to the number of bound fluorophores, and sometimes the intensity decreases. This effect is due to homo RET between the fluorophores, which decreases the quantum yield. Proximity of heavily labeled biomolecules to SIFs can result in increased intensities and apparently less quenching due to homo RET.[51–53] One example is shown in Figure 25.28 for immunoglobulin G (IgG) labeled with fluorescein.[53] As the labeling ratio is increased the intensity per fluorescein molecule decreases. This effect is due to homo RET between the fluoresceins, which decreases the quantum yield. The anisotropy values (insert) also decrease with increasing labeling ratio, which indicates that RET has occurred. Figure 25.29 shows that the intensity per fluorescein residue can increase as much as 40-fold for heavily labeled samples near SIFs. The release of self-quenching appears to be a general result[51–53] that suggests its use with any surface-bound assay.

25.7.3. Effect of Silver Particles on RET

Resonance energy transfer occurs over relatively large distances up to 100 Å. This distance is comparable to the size of large proteins and some protein assemblies. However, there are instances where RET over larger distances is

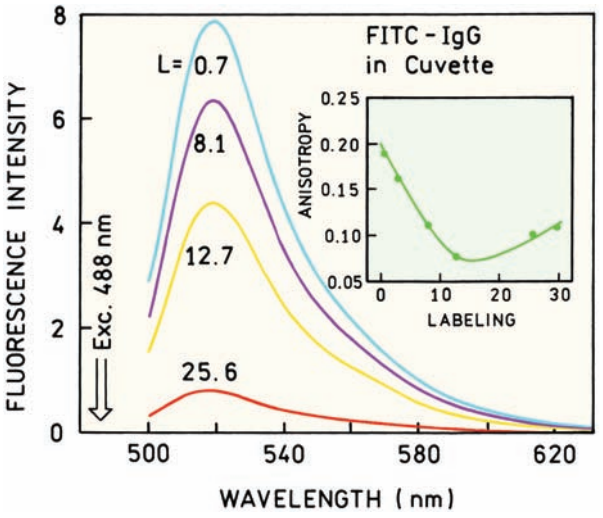

Figure 25.28. Emission spectra of fluorescein-labeled IgG. The numbers indicate the molar ratio of fluorescein to IgG. The intensities were measured for solutions with the same optical density for fluorescein. From [53].

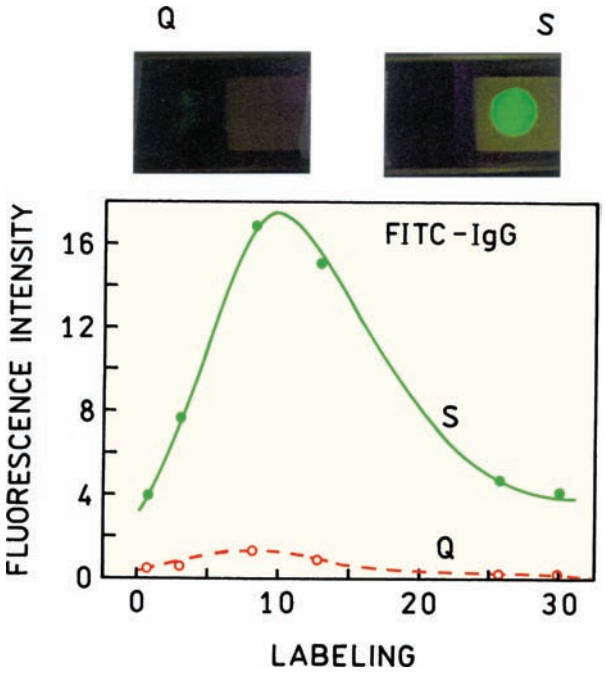

Figure 25.29. Photograph and relative intensities of fluorescein-labeled IgG on glass (Q) and SIFs (S). From [53].

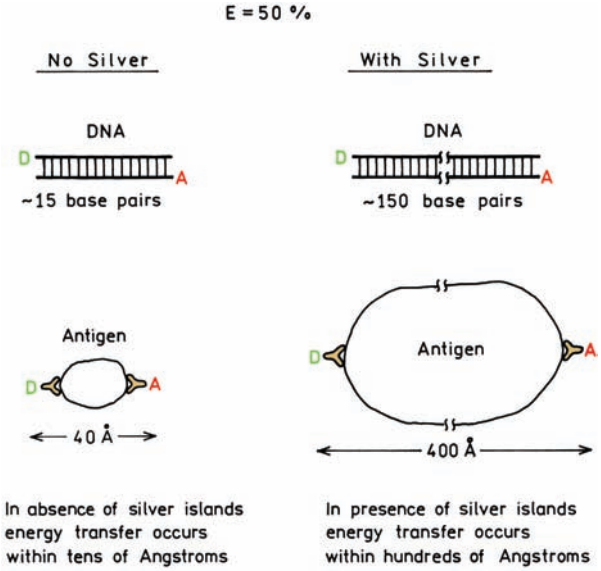

Figure 25.30. RET in the presence and absence of metallic particles.

desirable. One example is RET immunoassays (Figure 25.30). Fluorescence immunoassays are widely used, typically polarization as ELISA assays. Immunoassays are not usually performed using RET. This absence is probably due to the fact that in a sandwich assay the sizes of the antigen and antibodies are too large for RET to occur. Similarly, RET can be used to measure DNA hybridization if the donor and acceptor are within about 15 base pairs, but will not occur if the donor and acceptor are spaced by a much larger number of base pairs.

A small number of experiments have indicated that proximity to metal particles can increase the extent of energy transfer.[54–56] The effect of SIFs on RET was studied using a double-stranded DNA oligomer labeled with AMCA as the donor and Cy3 as the acceptor (Figure 25.31). The distance between the donor and acceptor was chosen so that the extent of energy transfer was small in the absence of single particles. The DNA oligomers labeled with both donor and acceptor were placed either near a single island film or between two SIFs. The RET efficiency was not affected by a single SIF, but was increased when the D–A pair was between two SIFs. The increase in RET can be seen from the increase in acceptor intensity near 570 nm. This result suggests that RET can be used to measure association reactions between large molecules or assemblies by passing the molecules between two layers of silver particles.

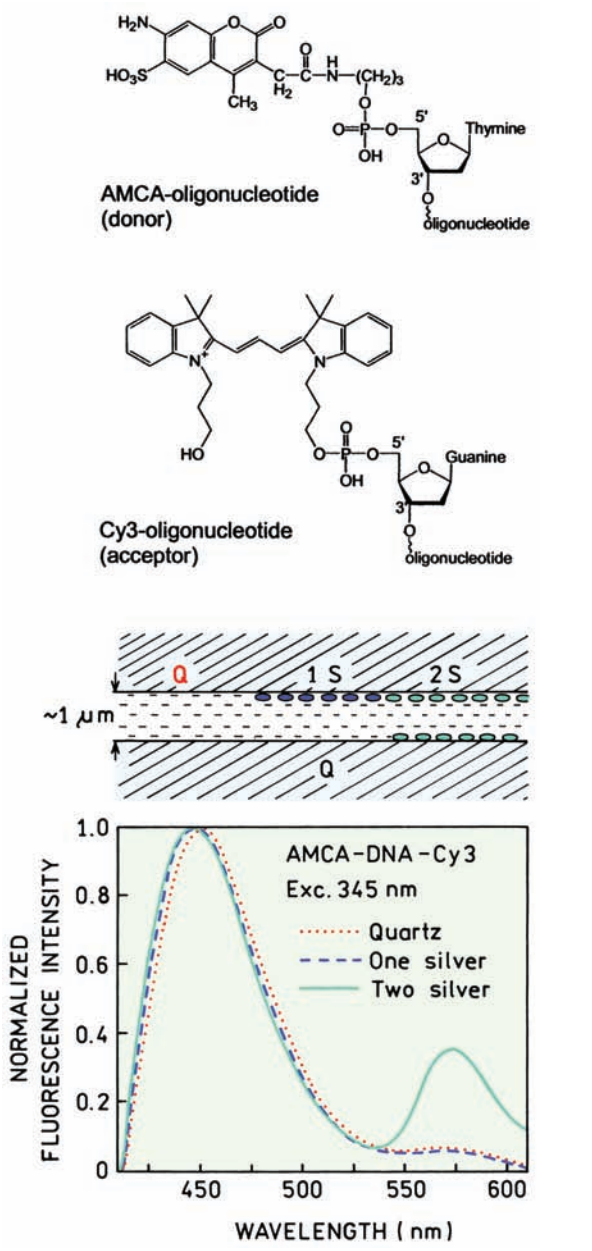

Figure 25.31. Effect of one or two SIFs on RET between AMCA and Cy3 bound to DNA. From [56].

25.8. MECHANISM OF MEF

In the preceding sections we described experiments that were all consistent with an increase in the radiative decay rate. However, some preparations of metal particles do not result in enhanced fluorescence. It is important to know

what types of particles are most effective for MEF and the properties of these particles that result in metal-enhanced fluorescence. We have developed a conceptually simple model that we hope has predictive value for MEF.[57] Mie theory can be used to calculate the optical properties of metal colloids when the colloids are smaller than the incident wavelength. These calculations show that the extinction of colloids is due to both light absorption and light scattering. The relative contribution of absorption and scattering depends on the size and shape of the colloids. In general, larger particles and non-spherical particles show larger relative contributions of scatter to the total extinction. At present we believe the scattering contribution of the total extinction is the origin of MEF. The scattering component represents far-field radiation from the induced oscillating dipole. In a sense this effect is similar to emission. This similarity can be seen in Figure 25.10, where the scattered light appears to be visually similar to fluorescence. It seems logical that the excited fluorophore and nearby metal particle cooperate in producing far-field radiation at the emission wavelength. We refer to this concept as the radiating plasmon (RP) model.[57] If correct, the RP model provides a rational approach for the design of metal particles for MEF. The particle or structure should be selected for a high cross-section for scattering and for a scattering component that is dominant over the absorption.

25.9. PERSPECTIVE ON RET

At present relatively few laboratories are performing studies on MEF.[58–65] The early results are confirming the results from our laboratory. If this trend continues MEF will become widely used in sensing, biotechnology, and forensics. The studies described in this chapter were performed using SIFs, which have a heterogeneous distribution of particle sizes. In the future we can expect MEF to use better-defined particles. Silver and gold colloids can be made with a variety of shapes,[66–79] some of which may be more useful for MEF. And, finally, it seems likely that MEF will be performed using regular particulate surfaces of a type prepared using nanosphere lithography,[80–82] dip-pen lithography,[83] microcontact printing,[84] and other emerging methods for nanolithography.

Our vision for the future of RDE is shown in Figure 25.32. At present almost all fluorescence experiments are performed using the free-space emission. This emission is mostly isotropic and the radiative decay rates are mostly constant (top). The use of RDE will allow the design of metallic structures that interact with the excited fluorophore. These interactions can result in modified spectral properties and directional emission (bottom). In some cases the directionality will be the result of the excited fluorophores creating plasmons in the metal, which in turn result in far-field radiation. The ability to control the emission process represents a paradigm shift for the field of fluorescence spectroscopy.

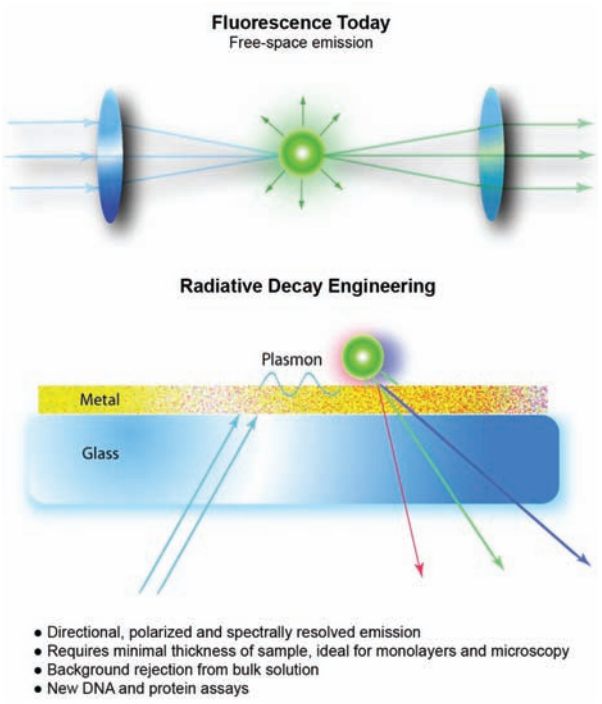

Figure 25.32. Comparison of free-space fluorescence emission with emission modified and directed by metallic structures.

REFERENCES

1. Strickler SJ, Berg RA. 1962. Relationship between absorption intensity and fluorescence lifetimes of molecules. *J Chem Phys* **37**:814–822.
2. Toptygin D, Savtchenko RS, Meadow ND, Roseman S, Brand L. 2002. Effect of the solvent refractive index on the excited state lifetime of a single tryptophan residue in a protein. *J Phys Chem B* **106**(14):3724–3734.
3. Ford GW, Weber WH. 1984. Electromagnetic interactions of molecules with metal surfaces. *Phys Rep* **113**:195–287.
4. Chance RR, Prock A, Silbey R. 1978. Molecular fluorescence and energy transfer near interfaces. *Adv Chem Phys* **37**:1–65.
5. Axelrod D, Hellen EH, Fulbright RM. 1992. Total internal reflection fluorescence. In *Topics in Fluorescence Spectroscopy*, Vol. 3: *Biochemical applications*, pp. 289–343. Ed JR Lakowicz. Plenum Press, New York.

6. Lakowicz JR, 2001. Radiative decay engineering: biophysical and biomedical applications. *Anal Biochem* **298**:1–24.
7. Das P, Metju H. 1985. Enhancement of molecular fluorescence and photochemistry by small metal particles. *J Phys Chem* **89**:4680–4687.
8. Gersten J, Nitzan A. 1981. Spectroscopic properties of molecules interacting with small dielectric particles. *J Chem Phys* **75**(3):1139–1152.
9. Weitz DA, Garoff S, Gersten JI, Nitzan A. 1983. The enhancement of Raman scattering, resonance Raman scattering, and fluorescence from molecules absorbed on a rough silver surface. *J Chem Phys* **78**(9):5324–5338.
10. Chew H. 1987. Transition rates of atoms near spherical surfaces. *J Chem Phys* **87**(2):1355–1360.
11. Kummerlen J, Leitner A, Brunner H, Aussenegg FR, Wokaun A. 1993. Enhanced dye fluorescence over silver island films: analysis of the distance dependence. *Mol Phys* **80**(5):1031–1046.
12. Philpott MR. 1975. Effect of surface plasmons on transitions in molecules. *J Chem Phys* **62**(5):1812–1817.
13. Amos RM, Barnes WL. 1997. Modification of the spontaneous emission rate of Eu^{3+} ions close to a thin metal mirror. *Phys Rev B* **55**(11):7249–7254.
14. Barnes WL. 1998. Fluorescence near interfaces: the role of photonic mode density. *J Mod Opt* **45**(4):661–699.
15. Amos RM, Barnes WL. 1999. Modification of spontaneous emission lifetimes in the presence of corrugated metallic surfaces. *Phys Rev B* **59**(11):7708–7714.
16. Drexhage KH. 1974. Interaction of light with monomolecular dye lasers. In *Progress in optics*, pp. 161–232. Ed E Wolfe. North-Holland Publishing, Amsterdam.
17. Weitz DA, Garoff S, Hanson CD, Gramila TJ. 1982. Fluorescent lifetimes of molecules on silver-island films. *Opt Lett* **7**(2):89–91.
18. Kerker M. 1985. The optics of colloidal silver: something old and something new. *J Colloid Interface Sci* **105**:297–314.
19. Faraday M. 1857. The Bakerian Lecture: experimental relations of gold (and other metals) to light. *Philos Trans* **147**:145–181.
20. Link S, El-Sayed MA. 2000. Shape and size dependence of radiative, non-radiative and photothermal properties of gold nanocrystals. *Int Rev Phys Chem* **19**:409–453.
21. Kreibig U, Vollmer M. 1995. *Optical properties of metal clusters*. Springer, New York.
22. Link S, El-Sayed MA. 1999. Spectral properties and relaxation dynamics of surface plasmon electronic oscillations in good and silver nanodots and nanorods. *J Phys Chem B* **103**:8410–8426.
23. Murphy CJ, Jana NR. 2002. Controlling the aspect ratio of inorganic nanorods and nanowires. *Adv Mater* **14**(1):80–83.
24. Yguerabide J, Yguerabide EE. 1998. Light scattering submicroscopic particles as highly fluorescent analogs and their use as tracer labels in clinical and biological applications, I: theory. *Anal Biochem* **262**(2):137–156.
25. Yguerabide J, Yguerabide EE. 1998. Light scattering submicroscopic particles as highly fluorescent analogs and their use as tracer labels in clinical and biological applications, II: experimental characterization. *Anal Biochem* **262**(2):157–176.
26. Yguerabide J, Yguerabide EE. 2001. Resonance light scattering particles as ultrasensitive labels for detection of analytes in a wide range of applications. *J Cell Biochem Suppl* **37**:71–81.
27. Schultz S, Mock J, Smith DR, Schultz DA. 1999. Nanoparticle based biological assays. *J Clin Ligand Assay* **22**(2):214–216.
28. Bauer G, Voinov S, Sontag G, Leitner A, Aussenegg FR, Pittner F, Schalkhammer T. 1999. Optical nanocluster microchips for human diagnostics. *SPIE Proc* **3606**:40–45.
29. Bauer G, Pittner F, Schalkhammer Th. 1999. Metal nano-cluster biosensors. *Mikrochim Acta* **131**:107–114.
30. Stich N, Gandhum A, Matushin V, Mayer C, Bauer G, Schalkhammer T. 2001. Nanofilms and nanoclusters: energy courses driving fluorophores of biochip bound labels. *J Nanosci Nanotechnol* **1**(4):397–405.
31. Taton TA, Mirkin CA, Letsinger RL. 2000. Scanometric DNA array detection with nanoparticle probes. *Science* **289**:1757–1760.
32. Reichert J, Csáki A, Köhler M, Fritzsche W. 2000. Chip-based optical detection of DNA hybridization by means of nanobead labeling. *Anal Chem* **72**:6025–6029.
33. Nam J-M, Thaxton CS, Mirkin CA. 2003. Nanoparticle-based bio-bar codes for the ultrasensitive detection of proteins. *Science* **301**: 1884–1886.
34. Gersten JI, Nitzan A. 1984. Accelerated energy transfer between molecules near a solid particle. *Chem Phys Lett* **104**(1):31–37.
35. Hua XM, Gersten JI, Nitzan A. 1985. Theory of energy transfer between molecules near solid state particles. *J Chem Phys* **83**: 3650–3659.
36. Lakowicz JR, Shen Y, D'Auria S, Malicka J, Fang J, Gryczynski Z, Gryczynski I. 2002. Radiative decay engineering, 2: effects of silver island films on fluorescence intensity, lifetimes and resonance energy tranfser. *Anal Biochem* **301**:261–277.
37. Malicka J, Gryczynski I, Maliwal BP, Fang J, Lakowicz JR. 2003. Fluorescence spectral properties of cyanine dye labeled DNA near metallic silver particles. *Biopolymers* **72**:96–104.
38. Malicka J, Gryczynski I, Fang J, Lakowicz JR. 2003. Fluorescence spectral properties of cyanine dye-labeled DNA oligomers on surfaces coated with silver particles. *Anal Biochem* **317**:136–146.
39. Lakowicz JR, Malicka J, Gryczynski I. 2003. Increased intensities of YOYO-1-labeled DNA oligomers near silver particles. *Photochem Photobiol* **77**(6):604–607.
40. Lakowicz JR, Malicka J, Gryczynski I. 2003. Silver particles enhance emission of fluorescent DNA oligomers. *BioTechniques* **34**(1):62–66.
41. Malicka J, Gryczynski I, Geddes CD, Lakowicz JR. 2003. Metal-enhanced emission from indocyanine green: a new approach to *in vivo* imaging. *J Biomed Opt* **8**(3):472–478.
42. Parfenov A, Gryczynski I, Malicka J, Geddes CD, Lakowicz JR. 2003. Enhanced fluorescence from fluorophores on fractal silver surfaces. *J Phys Chem* **107**:8829–8833.
43. Geddes CD, Cao H, Gryczynski I, Gryczynski Z, Fang J, Lakowicz JR. 2003. Metal-enhanced fluorescence (MEF) due to silver colloids on a planar surface: potential applications of indocyanine green to in vivo imaging. *J Phys Chem A* **107**:3443–3449.
44. Lakowicz JR, Shen B, Gryczynski Z, D'Auria S, Gryczynski I. 2001. Intrinsic fluorescence from DNA can be enhanced by metallic particles. *Biochem Biophys Res Commun* **286**:875–879.
45. Malicka J, Gryczynski I, Gryczynski Z, Lakowicz JR. 2003. Effects of fluorophore-to-silver distance on the emission of cyanine-dye labeled oligonucleotides. *Anal Biochem* **315**:57–66.

46. Stich N, Mayer C, Bauer G, Schalkhammer T. 2001. DNA biochips based on surface-enhanced fluorescence (SEF) for high-throughput interaction studies. *SPIE Proc* **4434**:128–137.
47. Mayer C, Stich N, Schalkhammer T. 2001. Surface-enhanced fluorescence biochips using industrial standard slide format and scanners. *SPIE Proc* **4252**:37–46.
48. Lochner N, Lobmaier C, Wirth M, Leitner A, Pittner F, Gabor F. 2003. Silver nanoparticle enhanced immunoassays: one step real time kinetic assay for insulin in serum. *Eur J Pharm Biopharm* **56**: 469–477.
49. Lobmaier Ch, Hawa G, Götzinger M, Wirth M, Pittner F, Gabor F. 2001. Direct monitoring of molecular recognition processes using fluorescence enhancement at colloid-coated microplates. *J Mol Recognit* **14**:215–222.
50. Malicka J, Gryczynski I, Lakowicz JR. 2003. DNA hybridization assays using metal-enhanced fluorescence. *Biochem Biophys Res Commun* **306**:213–218.
51. Lakowicz JR, Malicka J, D'Auria S, Gryczynski I. 2003. Release of the self-quenching of fluorescence near silver metallic surfaces. *Anal Biochem* **320**:13–20.
52. Malicka J, Gryczynski I, Lakowicz JR. 2003. Enhanced emission of highly labeled DNA oligomers near silver metallic surfaces. *Anal Chem* **75**:4408–4414.
53. Lakowicz JR, Malicka J, Huang J, Gryczynski Z, Gryczynski I. 2004. Ultrabright fluorescein-labeled antibodies near silver metallic surfaces. *Biopolymers* **74**:467–475.
54. Lakowicz JR, Kusba J, Shen Y, Malicka J, D'Auria S, Gryczynski Z, Gryczynski I. 2003. Effects of metallic silver particles on resonance energy transfer between fluorophores bound to DNA. *J Fluoresc* **13**(1):69–77.
55. Malicka J, Gryczynski I, Kusba J, Lakowicz JR. 2003. Effects of metallic silver island films on resonance energy transfer between N,N'-(dipropyl)-tetramethyl-indocarbocyanine (Cy3)- and N,N'-(dipropyl)-tetramethyl-indodicarbocyanine (Cy5)-labeled DNA. *Biopolymers* **70**:595–603.
56. Malicka J, Gryczynski I, Fang J, Kusba J, Lakowicz JR. 2003. Increased resonance energy transfer between fluorophores bound to DNA in proximity to metallic silver particles. *Anal Biochem* **315**:160–169.
57. Lakowicz JR. 2004. Radiative decay engineering, 5: metal-enhanced fluorescence and plasmon emission. *Anal Biochem* **337**:171-194.
58. Sokolov K, Chumanov G, Cotton TM. 1998. Enhancement of molecular fluorescence near the surface of colloidal metal films. *Anal Chem* **70**:3898–3905.
59. Hayakawa T, Selvan ST, Nogami M. 1999. Field enhancement effect of small Ag particles on the fluorescence from Eu^{3+}-doped SiO_2 glass. *Appl Phys Lett* **74**(11):1513–1515.
60. Selvan ST, Hayakawa T, Nogami M. 1999. Remarkable influence of silver islands on the enhancement of fluorescence from Eu^{3+} ion-doped silica gels. *J Phys Chem B* **103**:7064–7067.
61. Vasilev K, Stefani FD, Jacobsen V, Knoll W. 2004. Reduced photobleaching of chromophores close to a metal surface. *J Chem Phys* **120**(14):6701–6704.
62. Aussenegg FR, Leitner A, Lippitsch ME, Reinisch H, Reigler M. 1987. Novel aspects of fluorescence lifetime for molecules positioned close to metal surfaces. *Surface Sci* **139**:935–945.
63. DeSaja-Gonzalez J, Aroca R, Nagao Y, DeSaja JA. 1997. Surface-enhanced fluorescence and SERRS spectra of *N*-octadecyl-3,4:9,10-perylenetetracarboxylic monoanhydride on silver island films. *Spectrochim Acta* **53**:173–181.
64. Wiederrecht GP, Wurtz GA, Im JS, Hranisavlievic J. 2004. J-aggregates on metal nanoparticles characterized through ultrafast spectroscopy and near-field optics. *Scanning* **26**(I):I-2/I-9.
65. Wiederrecht GP, Wurtz GA, Hranisavljevic J. 2004. Coherent coupling of molecular excitons to electronic polarizations of noble metal nanoparticles. *Nanotechnol Lett* **4**(11):2121–2125.
66. Sosa IO, Noguez C, Barrera RG. 2003. Optical properties of metal nanoparticles with arbitrary shapes. *J Phys Chem B* **107**:6269–6275.
67. Zhang J, Han B, Liu M, Liu D, Dong Z, Liu J, Li D. 2003. Ultrasonication-induced formation of silver nanofibers in reverse micelles and small-angle x-ray scattering studies. *J Phys Chem B* **107**:3679–3683.
68. Kim F, Song JH, Yang P. 2002. Photochemical synthesis of gold nanorods. *J Am Chem Soc* **124**:14316–14317.
69. Taub N, Krichevski O, Markovich G. 2003. Growth of gold nanorods on surfaces. *J Phys Chem B* **107**:11579–11582.
70. Jana NR, Gearheart L, Murphy CJ. 2001. Wet chemical synthesis of high aspect ratio cylindrical gold nanorods. *J Phys Chem B* **105**:40656–40667.
71. Chen S, Carroll DL. 2002. Synthesis and characterization of truncated triangular silver nanoplates. *Nanotechnol Lett* **2**(9):1003–1007.
72. Pham T, Jackson JB, Halas NJ, Lee TR. 2002. Preparation and characterization of gold nanoshells coated with self-assembled monolayers. *Langmuir* **18**:4915–4920.
73. Maillard M, Giorgio S, Pileni MP. 2003. Tuning the size of silver nanodisks with similar aspect ratios: synthesis and optical properties. *J Phys Chem B* **107**:2466–2470.
74. Wei G, Zhou HL, Liu ZG, Song YH, Wang L, Sun LL, Li Z. 2005. One-step synthesis of silver nanoparticles, nanorods, and nanowires on the surface of DNA network. *J Phys Chem B* **109**(18):8738–8743.
75. Ni CY, Hassan PA, Kaler EW. 2005. Structural characteristics and growth of pentagonal silver nanorods prepared by a surfactant method. *Langmuir* **21**(8):3334–3337.
76. Liu FK, Chang YC, Huang PW, Ko FH, Chu TC. 2004. Preparation of silver nanorods by rapid microwave heating. *Chem Lett* **33**(8): 1050–1051.
77. Lee GJ, Shin SI, Kim YC, Oh SG. 2004. Preparation of silver nanorods through the control of temperature and pH of reaction medium. *Mater Chem Phys* **84**(2–3):197-204.
78. Sharma J, Chaki NK, Mahima S, Gonnade RG, Mulla IS, Vijayamohanan K. 2004. Tuning the aspect ratio of silver nanostructures: the effect of solvent mole fraction and 4-aminothiophenol concentration. *J Mater Chem* **14**(6):970–975.
79. Hu JQ, Chen Q, Xie ZX, Han GB, Wang RH, Ren B, Zhang Y, Yang ZL, Tan ZW. 2004. A simple and effective route for the synthesis of crystalline silver nanorods and nanowires. *Adv Funct Mater* **14**(2): 183–189.
80. Whitney AV, Myers BD, Van Duyne RP. 2004. Sub-100 nm triangular nanopores fabricated with the reactive ion etching variant of nanosphere lithography and angle-resolved nanosphere lithography. *Nanotechnol Lett* **4**(8):1507–1511.

81. Haynes CL, McFarland AD, Smith MT, Hulteen JC, Van Duyne RP. 2002. Angle-resolved nanosphere lithography: manipulation of nanoparticle size, shape, and interparticle spacing. *J Phys Chem B* **106**(8):1898–2002.
82. Jensen TR, Malinsky MD, Haynes CL, Van Duyne RP. 2000. Nanosphere lithography: tunable localized surface plasmon resonance spectra of silver nanoparticles. *J Phys Chem B* **104**(45): 10549–10556.
83. Choi D-G, Kim S, Lee E, Yang S-M. 2005. Particle arrays with patterned pores by nanomatching with colloidal masks. *J Am Chem Soc* **127**:1636–1637.
84. Ormonde AD, Hicks ECM, Castillo J, Van Duyne RP. 2004. Nanosphere lithography: fabrication of large-area Ag nanoparticle arrays by convective self-assembly and their characterization by scanning UV-visible extinction spectroscopy. *Langmuir* **20**:6927-6931.

PROBLEM

P25.1. *Calculation of the Quantum Yield and Increase in Radiative Rate Near an SIF*. Figure 25.16 shows the emission spectra of rose bengal (RB) in solution and between SIFs. Assume all the molecules are affected equally by the SIF. What is the relative increase in the radiative decay rate (Γ) due to the SIF? Assume the natural radiative lifetime in the absence of metals is 4 ns. Also assume the excitation rate and the non-radiative decay rates are the same in the presence and absence of the SIF.

Now assume that only 10% of the RB molecules are affected by the SIF. What are the quantum yield and relative increased in Γ due to the SIF?